Doping at the Mn site of the electron-doped manganite $Ca_{0.9}Ce_{0.1}MnO_3$

2002 J. Phys.: Condens. Matter 14 9039

(http://iopscience.iop.org/0953-8984/14/39/313)

INSTITUTE OF PHYSICS PUBLISHING JOURNAL OF PHYSICS: CONDENSED MATTER

J. Phys.: Condens. Matter **14** (2002) 9039–9052 PII: S0953-8984(02)38755-1

Doping at the Mn site of the electron-doped manganite $Ca_{0.9}Ce_{0.1}MnO_3$

R Ganguly[1], **M Hervieu, A Maignan, C Martin and B Raveau**

Laboratoire CRISMAT, ISMRA, 6 Boulevard du Maréchal Juin, 14050 CAEN Cedex, France

E-mail: rajibg@magnum.barc.ernet.in

Received 17 July 2002, in final form 2 August 2002
Published 19 September 2002
Online at stacks.iop.org/JPhysCM/14/9039

Abstract

The effects of substitution of chromium and ruthenium for manganese on the magnetic and transport properties of electron-doped manganite $Ca_{0.9}Ce_{0.1}MnO_3$, with d_z^2 orbital-ordered and the associated antiferromagnetic (AFM) characters, have been studied. As expected, due to the participation of the $Cr^{3+}(t_{2g}^3\ e_g^0)$ and $Ru^{4+/5+}[t_{2g}^4\ e_g^0/t_{2g}^3\ e_g^0)]$ ions in the e_g band broadening for the $Mn^{3+}(t_{2g}^3\ e_g^1)$ and $Mn^{4+}(t_{2g}^3\ e_g^0)$ species, the suppression of the AFM transition by Ru and Cr doping is accompanied by an increase in the ferromagnetic (FM) character. The coexistence of FM and AFM phases in these Ru- and Cr-substituted compounds leads to the observations of cluster glass behaviour, the giant magneto-resistive memory (GMM) effect and other magnetic-history-dependent magnetic and transport properties. Our observation of the GMM effect in these Cr- and Ru-doped compounds is the first of its kind in the magnetically phase-separated bulk polycrystalline compounds.

1. Introduction

Discoveries of colossal magnetoresistance (CMR) and a rich variety of other physical properties [1–9] in the hole- and the electron-doped manganites have created a renewed interest of the researchers in these classes of compounds. Recent studies [10–15] revealed that the ferromagnetic (FM) and metallic characters induced by hole and electron doping, respectively, are significantly different in nature. Unlike the hole-doped manganites, the electron-doped manganites show FM behaviour in a very narrow range of carrier concentration with an unusual effect of the variation of r_A (the average size of the ions at the rare earth site) on their physical properties [10, 11]. Ferromagnetism in the electron-doped, $Ln_{1-x}Ca_xMnO_3$ (Ln = rare earth, $x > 0.5$) compounds always coexists with competing G-type or C-type AFM phases, leading to the observation of cluster-glass-type behaviour even in the compounds with long range FM order [12–15]. Furthermore, whereas the hole-doped, $Ln_{1-x}Ca_xMnO_3$ ($x \leqslant 0.5$)

[1] Present address: Novel Materials and Structural Chemistry Division, BARC, Mumbai-400 085, India.

compounds show semiconducting behaviour in their paramagnetic state, a metallic behaviour is exhibited by the electron-doped compounds ($x > 0.5$) above their FM/AFM transition temperatures [13–15]. This behaviour of the electron-doped compounds has been attributed to the decreased binding energy of the polarons in the presence of a reduced number of J–T-distorted Mn^{3+} ions [14, 15].

The AFM and charge ordering (CO) states of the hole-doped and electron-doped manganites can be destroyed by the substitutions of transition or non-transition metal ions for Mn. The substitutions of a number of transition metal ions like Cr^{3+}, Co^{2+}, Ni^{2+} and $Ru^{4+/5+}$ also play important roles in inducing FM and CMR properties in various AFM and CO manganites [16–22]. It has been shown that the transition-metal-substituted 'AFM' or 'CO' manganites show signatures of coexistence of the FM and the orbital-ordered (OO)/(CO) AFM phases, with or without the same crystallographic structure [19–22]. According to recent literature reports [23–29], these, as well as other magnetically phase-separated systems, exhibit an interesting set of magnetic-history-dependent magnetic and transport properties. As has been explained in the literature, such magnetic history dependence arises from the influence of the magnetic field on the relative stability of the FM phase with respect to the AFM phase.

In this paper, we report a detailed study on the physical properties of the electron-doped manganites, $Ca_{0.9}Ce_{0.1}Mn_{1-y}M_yO_3$ (M = Ru, Cr). In view of the limited phase stability ($x \leqslant 0.2$) [30], and higher AFM transition temperatures observed in the $Ca_{1-x}Ce_xMnO_3$ compounds than in the $Ca_{1-2x}Sm_{2x}MnO_3$ compounds [10], mainly due to the size difference between the Sm^{3+} and Ce^{4+} ions, the studies were aimed at comparing these properties with those reported for the $Ca_{0.8}Sm_{0.2}Mn_{1-y}M_yO_3$ (M = Ru, Cr) compounds [18, 20]. We also show how the coexistence of the FM and AFM phases in the present Cr- and Ru-substituted compounds leads to the observations of the giant magnetic memory (GMM) effect and other magnetic-history-dependent magnetic and transport properties. To the best of our knowledge observation of such a huge magnetic memory effect is reported for the first time in the magnetically phase-separated polycrystalline manganites.

2. Experimental details

The samples of nominal compositions $Ca_{0.9}Ce_{0.1}Mn_{1-y}M_yO_3$ ($y = 0.05$, 0.10 and M = Cr, Ru) were prepared by solid state reaction in air between $CaCO_3$, CeO_2, MnO_2, Cr_2O_3 and RuO_2 at 1500 °C. The room temperature x-ray diffraction (XRD) patterns of the compounds were taken in a Philips diffractometer, using Cu Kα radiation. Electron diffraction (ED) studies on the $Ca_{0.9}Ce_{0.1}MnO_3$ compound at room temperature and at 92 K were carried out using a JEOL 2010 electron microscope, equipped with an energy dispersive spectroscopy (EDS) analyser. Sample for this purpose was prepared first by dispersing the crystallites in alcohol, and then by depositing the dispersed particles on a holey carbon film supported by a Cu grid. Numerous crystallites were characterized and analysed by reconstructing the reciprocal space and tilting them around the crystallographic axes. Four-probe resistivity measurements in the temperature range from 5 to 400 K at 0 and 7 T magnetic fields were carried out using a Quantum Design physical property measurement system. AC and DC magnetic measurements were carried out using a Quantum Design SQUID magnetometer (5 K $\leqslant T \leqslant$ 400 K).

3. Results and discussion

The Rietveld refinements of the room temperature XRD patterns show that the samples of all the compositions form single-phase compounds with orthorhombically distorted perovskite

Table 1. The values of the lattice parameters, the activation energy for conduction (E_a), characteristic relaxation time (τ') and the dispersion parameter (β) of the compounds $Ca_{0.9}Ce_{0.1}Mn_{1-y}M_yO_3$ (M = Cr, Ru; $y = 0.00$, 0.05 and 0.10).

'y'	A (Å)	b (Å)	c (Å)	E_a (meV)	τ' (at 5 K) (s)	β (at 5 K)
0.00	5.3209(5)	7.5150(8)	5.3763(6)	15.16	—	—
0.05 (Cr)	5.3102(5)	7.5212(9)	5.3533(5)	29.03	3.67×10^6	0.114
0.10 (Cr)	5.3205(7)	7.519(9)	5.3592(5)	33.59	—	—
0.05 (Ru)	5.2988(4)	7.501(1)	5.3345(6)	45.79	7.85×10^7	0.106
0.10 (Ru)	5.3055(6)	7.513(8)	5.3470(5)	55.49	—	—

Table 2. The six-co-ordinated ionic radius values of different ions.

Ion	Size (Å)	Ion	Size (Å)	Ion	Size (Å)
Mn^{3+}	0.645	Ru^{4+}	0.620	Cr^{3+}	0.615
Mn^{4+}	0.530	Mn^{5+}	0.565	Cr^{4+}	0.550

structure (*Pnma* space group), the lattice parameters of which are shown in table 1. This shows that the orthorhombic structure of $Ca_{0.9}Ce_{0.1}MnO_3$ is stable up to 10% Cr and Ru substitution. When substituted for Mn, the Cr ions remain in the trivalent state, but the Ru ions, with a Ru^{4+}/Ru^{5+} mixed valence, probably lead to the partial conversion of Mn^{4+} ions to the Mn^{3+} ions, governed by the equation $Mn^{4+} + Ru^{4+} = Ru^{5+} + Mn^{3+}$ [31]. The observed absence of any systematics of the lattice parameters with increase in the substituent ion concentrations arises due to the small difference in size between the above mentioned probable substituted and substituent ions (table 2) [32], and due to only small values of the level of substitutions (up to 10%). The magnetization versus temperature plots of the compounds recorded at 5 T magnetic field are shown in figure 1. The parent compound ($y = 0.0$) shows a paramagnetic to AFM transition at about 170 K. Hysteresis observed between the field-cooled (FC) and field-warmed (FW) magnetization plots indicates that the transition is of first order. Zeng *et al* [30] suggested that the observed AFM transition is associated with long range CO. However, studies on the compounds $Ca_{0.8}Sm_{0.2}MnO_3$ and $Ca_{0.9}Th_{0.1}MnO_3$, with the same Mn^{4+} content as $Ca_{0.9}Ce_{0.1}MnO_3$, and with similar paramagnetic to AFM transitions, suggested that the AFM state in these is not associated with CO, but with one-dimensional d_z^2 orbital polarization, often described as an orbital ordering (OO) [33–35]. ED patterns of these compounds recorded at 92 K, below the AFM transition temperature, did not show any superlattice reflections associated with long range CO [33–35]. Instead, it has been shown that their C-type AFM state has monoclinically distorted perovskite structure, associated with the d_z^2 OO. ED studies carried out by us on $Ca_{0.9}Ce_{0.1}MnO_3$ at 92 K also show that the room temperature orthorhombically distorted perovskite structure (*Pnma* space group) of this compound changes to a monoclinically distorted perovskite one ($P2_1/m$ space group) at 92 K. A typical [010] ED pattern recorded at 92 K (figure 2) shows the splitting of the reflections characteristic of a monoclinic cell, $a \approx a_p\sqrt{2}$, $b \approx 2a_p$, $c \approx a_p\sqrt{2}$ and $\beta = 90° + \varepsilon$, and space group $P2_1/m$. The two white lines making an angle of '2ε' are drawn for easier detection of the monoclinic distortion. The electron microscopy images evidence the existence of twinning domains, as previously reported for the C-type AFM phase of the $Ca_{1-2x}Sm_{2x}MnO_3$ compounds [33]. Thus comparing these results with those reported for the $Ca_{0.8}Sm_{0.2}MnO_3$ and $Ca_{0.9}Th_{0.1}MnO_3$ compounds, we suggest that, as against the claim made by Zeng *et al* [30], the AFM state in the $Ca_{0.9}Ce_{0.1}MnO_3$ compound is associated with 'OO' and not with 'CO'.

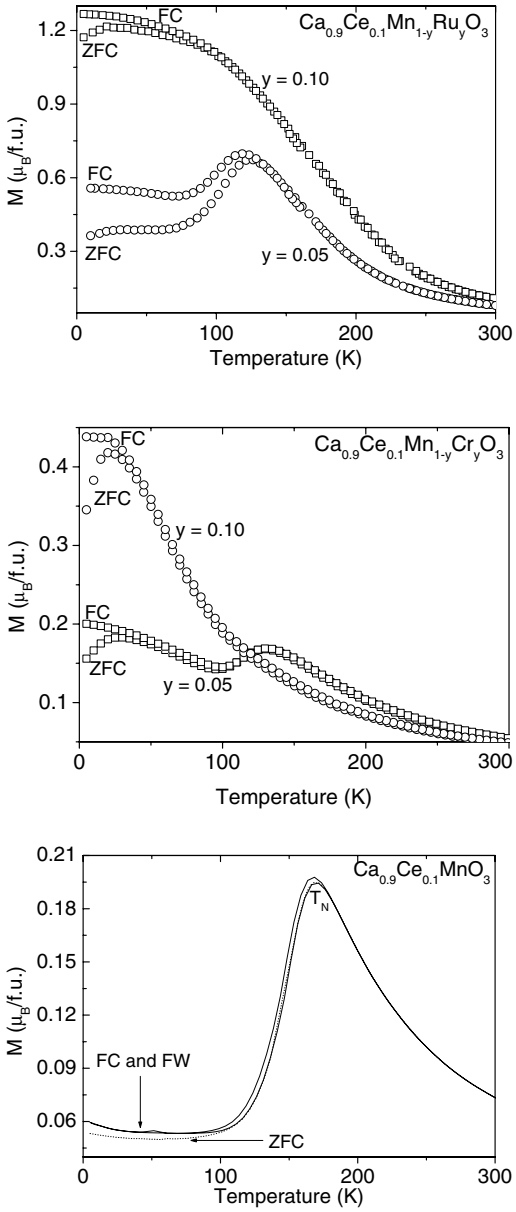

Figure 1. DC magnetization versus temperature plots for the $Ca_{0.9}Ce_{0.1}Mn_{1-y}M_yO_3$ (M = Cr, Ru, $y = 0.00$, $y = 0.05$ and 0.10) compounds, recorded at 5 T magnetic field, under FC and ZFC conditions.

As shown in figure 1, substitutions of both Cr and Ru weaken the paramagnetic to AFM transitions, but simultaneously enhance the magnetic signal indicative of the presence of growing FM phases with increase in the level of substitution. The observed drop in magnetization for both the Cr- and Ru-substituted $y = 0.05$ compounds indicates the presence of the AFM phase along with that of the FM phase. Considering that Cr and Ru ions remain in the trivalent and pentavalent state, respectively (as discussed in the last paragraph) [31],

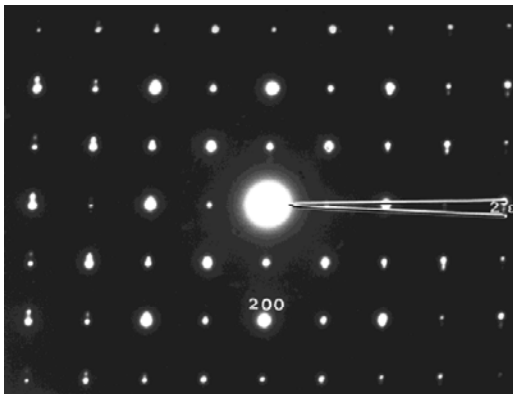

Figure 2. ED pattern of $Ca_{0.9}Ce_{0.1}MnO$, recorded at 92 K, showing monoclinic distortion in the perovskite structure.

and according to the phase diagram reported for $Sm_{1-x}Ca_xMnO_3$ [15], the change in valence of the Mn ions upon substitution of Cr and Ru cannot lead to Mn ion valence favouring FM correlation. As has been suggested in the literature [31], AFM and FM exchange interactions of the Mn ions with the Cr and Ru ions, respectively, play a role in breaking the AFM alignments of the manganese spins leading to their FM alignment. Substitutions of Cr and Ru in the $Ca_{0.8}Sm_{0.2}MnO_3$ compound also show similar behaviours with suppression of AFM character and enhancement of FM characters occurring simultaneously [18, 20]. Detailed ED studies carried out at 92 K on the $Ca_{0.8}Sm_{0.2}Mn_{1-y}Ru_yO_3$ compounds showed that the suppression of the AFM transition by Ru doping is also associated with a decrease in the monoclinic distortion as well as a decrease in the monoclinic phase fraction [19]. From the enhanced FM signal with increase in the Ru concentration and the presence of the monoclinic phase up to $y = 0.06$, it has been suggested that C-type AFM phases and the FM phases coexist in those Ru-doped compounds with compositions up to $y = 0.06$ [19]. The presence of two magnetic transitions in the AC-susceptibility versus temperature behaviour of the $y = 0.10$ compound, on the other hand, has been explained on the basis of coexistence of the G-type AFM and FM phases with the same orthorhombic structure [31]. Figure 1 shows that all the Cr- and Ru-doped compounds in the present case exhibit significant thermo-magnetic irreversibilities, although the magnetizations were measured at a field as high as 5 T. Since these compounds, especially the Ru-doped compounds, show a very low value of coercive field (H_C) (figure 3), such large thermomagnetic irreversibilities at the high measuring field of 5 T are clearly not due to large domain wall pinning. Rather they are likely to arise from the coexistence of the FM and the AFM phases, with the growth of the FM phases being favoured while cooling the compounds under magnetic field. The subtle balance between the FM and AFM phase fractions in these Cr- and Ru-doped compounds, thus, can effectively be controlled by changing the history of magnetic field they are subjected to. A similar behaviour is also exhibited by the electron-doped compound, $Ca_{0.85}Sm_{0.15}MnO_3$, with low values of coercive field and with co-existing FM (orthorhombic) and C-type AFM (monoclinic) phases [23]. Neutron diffraction studies under magnetic field carried out on this compound [29] also confirm the magnetic-history-dependent changes in the phase fractions of the orthorhombic and monoclinic phase associated with FM and AFM alignment of spins, respectively.

Interesting effects of the coexistence of the FM and AFM phases in the Cr- and Ru-substituted compounds are also observed in their M versus H loops (figure 3). This is reflected

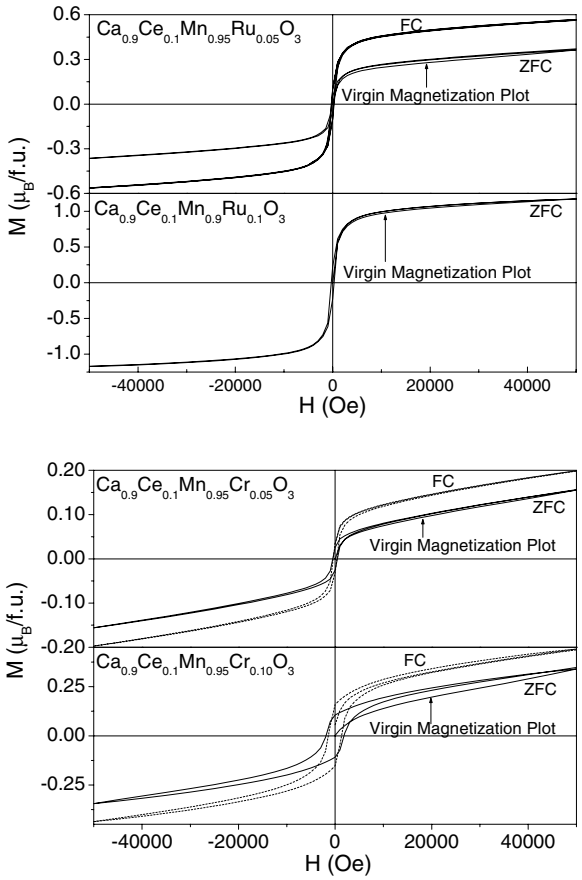

Figure 3. The M versus H plots of the $Ca_{0.9}Ce_{0.1}Mn_{1-y}M_yO_3$ (M = Cr, Ru; $y = 0.05$ and 0.10) compounds recorded at 5 K.

in the unusual position of the virgin magnetization plot with respect to the loop area as it lies almost completely outside the M–H loops. The effect is more prominent in the case of Cr-substituted compounds than in the case of the Ru-substituted compounds. Such a behaviour, which is indicative of an irreversible transformation of the magnetic phase by the application of magnetic field, when the 'virgin' magnetization curve is recorded, has been reported in the case of the hole-doped perovskite manganite, $Pr_{0.7}Ca_{0.25}Sr_{0.05}MnO_3$, with coexisting FM and AFM phases [36]. As in the case of the M–T plots these M–H plots also show higher magnetizations when measurements were made after cooling under 5 T. Similar to what is observed in the case of the other electron-doped compounds [12–14], due to the presence of AFM phases along with the FM phases, the magnetization values of the present compounds at 5 T are much less than the maximum magnetization achievable theoretically ($\approx 3.2\ \mu_B$). An increase in magnetization at 5 K and 5 T magnetic field shows that the FM phase fraction increases with increase in the Cr and Ru ion concentrations.

Since the frequency dependence of the AC-susceptibility behaviour is known to reflect the dynamics of the short range FM clusters present in the magnetically phase-separated electron-doped manganites, $Ca_{0.9}Sm_{0.1}MnO_3$ [14], we measured the AC-susceptibility versus temperature behaviours of the Ru-doped $y = 0.05$ and 0.10 compounds at various frequencies

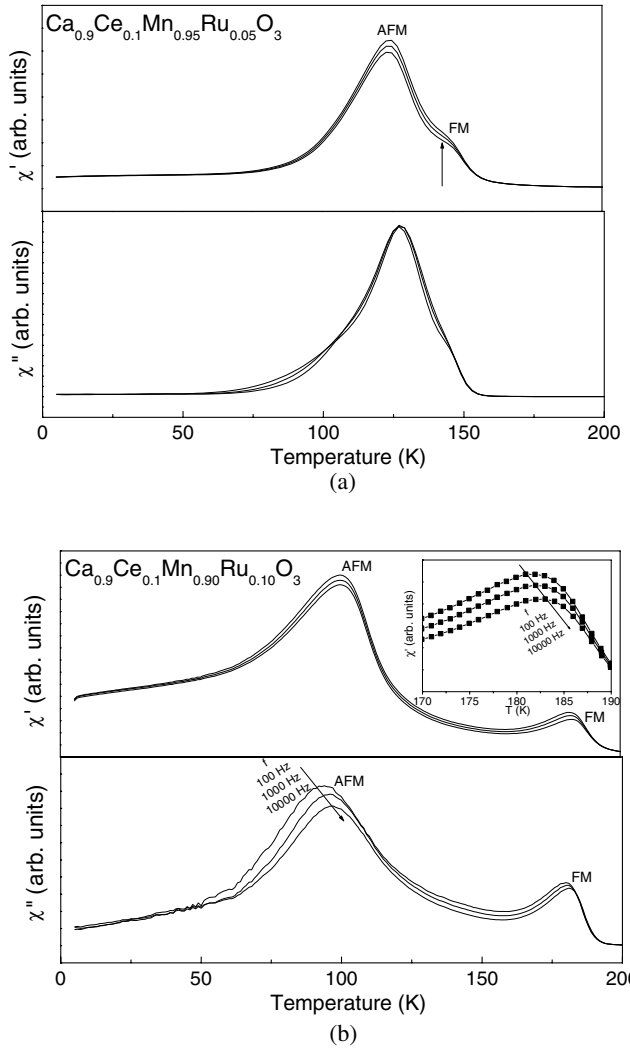

Figure 4. The AC-susceptibility versus temperature plots of $Ca_{0.9}Ce_{0.1}Mn_{0.95}Ru_{0.05}O_3$ and $Ca_{0.9}Ce_{0.1}Mn_{0.90}Ru_{0.10}O_3$ at different frequencies and at 10 Oe applied AC field.

(100, 1000, 10 000 Hz), at 10 Oe AC field, as shown in figure 4. For both the compounds, unlike in the case of the high field DC magnetization versus temperature plots, two transitions associated with the onset of FM and AFM characters are observed. Although the transition temperatures are different, the observed behaviours are similar to those observed in the case of the $Ca_{0.8}Sm_{0.2}Mn_{1-y}Ru_yO_3$ compounds. As has already been discussed, the two well separated peaks observed in the $y = 0.10$ compound arise from the coexistence of the FM and the G-type AFM phases with the same orthorhombically distorted perovskite structure [31]. The absence of similar double transitions in its DC magnetization versus temperature plots shows that the G-type AFM transition is suppressed under 5 T. Whereas their ZFC plots show drops in magnetization at very low temperature, the respective FC plots do not show any such drop down to 5 K. The OO C-type AFM phase and the G-type AFM phases present in the Ru-doped $y = 0.05$ and the 0.10 compounds, respectively, thus behave in a different way under the

influence of the magnetic field. Both the Ru-doped compounds show frequency dependence in their χ' versus temperature behaviours, below the respective FM transition temperatures. The observed frequency dependence is clearer in the case of the $y = 0.10$ compound (inset of figure 4(b)) and is marked with an 'arrow' for the $y = 0.05$ compound (figure 4(a)). The $y = 0.10$ compound also shows significant frequency dependence for both the peaks observed in its χ'' versus temperature behaviour. In the literature [14, 37–39], the frequency dependence observed in the χ' and χ'' versus temperature plots of various doped perovskite manganites and cobaltites has been explained on the basis of a cluster glass behaviour. It has been suggested that they arise from the relaxation of short-range FM clusters embedded in the AFM phases. The neutron diffraction study on $Ca_{0.9}Sm_{0.1}MnO_3$ [12] clearly shows that a significant amount of FM phase fraction does not contribute to the ordered moment in its neutron diffraction pattern and remains in the form of short range ordered clusters, separated by the majority AFM phases. The frequency dependence appears when the relaxation time of these short range clusters along the fluctuating ac field directions increases with a decrease in temperature and becomes of the order of the measurement times associated with applied frequencies (reciprocal of frequency). The AC-susceptibility versus temperature behaviour of the Ru-substituted compounds thus shows how the magnetic phase separation gives rise to cluster-glass-like behaviour. We will now discuss the effect of the magnetic phase separation on the resistivity versus temperature behaviours of the Cr- and Ru-doped compounds.

Figures 5 and 6 show the resistivity versus temperature plots of the compounds. As in the case of the magnetization versus temperature plots, hysteresis associated with change of slope of resistivity in the parent compound near the AFM transition temperature also suggests the first order nature of the transition. Application of a 7 T magnetic field weakens the AFM transition leading to the observation of a peak in magnetoresistance near the AFM transition temperature. The difference in the observed magnetoresistance behaviour from that reported by Zeng *et al* [30] probably arises from the difference in the synthesis procedure followed. A metal-like behaviour is observed in the paramagnetic region, similar to what has been observed in the $Ca_{0.9}Th_{0.1}MnO_3$ and $Ca_{0.8}Sm_{0.2}MnO_3$ compounds [10]. In the literature, from the observation of a much lower value of activation energy of thermopower than that of electrical resistivity, the resistivity behaviour in the paramagnetic region of the hole- and electron-doped manganites has been explained on the small polaron hopping mechanism, governed by the equation

$$\rho = AT \exp(E_a/kT)(A = \text{ constant })(\text{see [14–15, 40]}).$$

In the present case, the resistivity data for all the compounds in the paramagnetic region can be fitted quite well by this equation. Ru and Cr doping destroys the metallic character in the paramagnetic state due to an increase in the activation energy (E_a) (table 1). This behaviour is different from what is observed in the case of the $Ca_{0.8}Sm_{0.2}Mn_{1-y}Ru_yO_3$ compounds where the Ru-substituted compounds show a metallic behaviour in the paramagnetic region. As shown in figures 5 and 6, although doping of both Cr and Ru suppresses the AFM transition, insulator–metal (I–M) transition due to percolation of the FM phases is observed only for the Ru-substituted $y = 0.10$ compound, which shows a maximum FM signal. Both the Ru- and Cr-substituted $y = 0.05$ compounds show changes in the slope near their respective AFM transition temperatures observed from their DC magnetization plots. These two and the Cr-substituted $y = 0.10$ compound show CMR at low temperature with a value of $\rho_{(0\ \mathrm{T})}/\rho_{(7\ \mathrm{T})}$ as high as 10^6 in the case of the Ru-substituted $y = 0.05$ compound. The Ru- and the Cr-substituted $y = 0.05$ compounds also exhibit orders of magnitude difference between the FC and ZFC resistances, which have earlier been reported in the case of the magnetically phase-separated compound $Ca_{0.85}Sm_{0.15}MnO_3$ [23]. The CMR behaviour and the large difference between the ZFC and the FC magnetizations in $Ca_{0.85}Sm_{0.15}MnO_3$ have been explained on

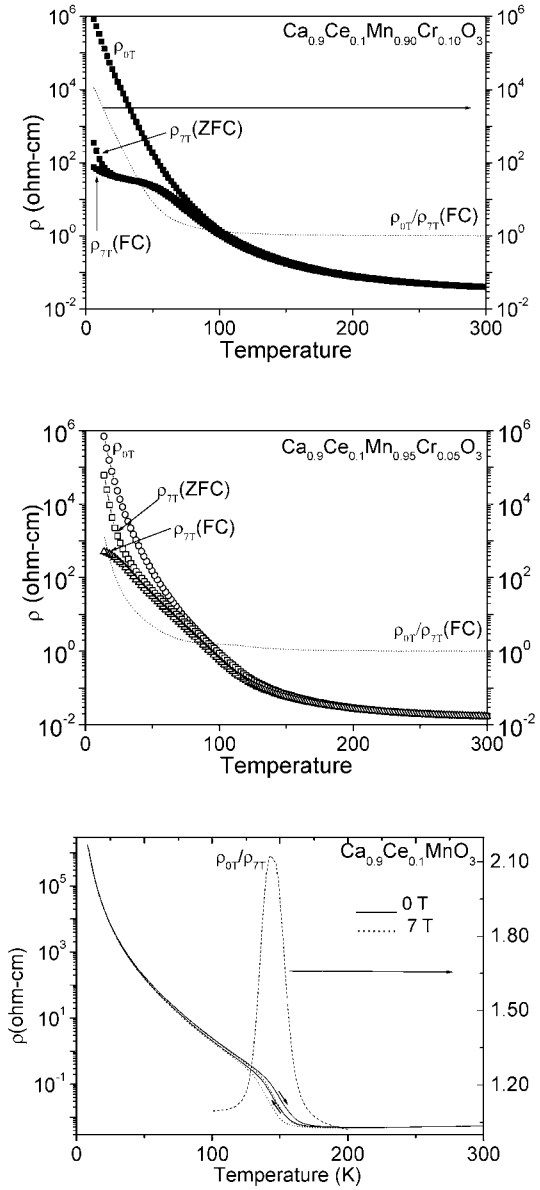

Figure 5. The DC electrical resistivity versus temperature plots of the $Ca_{0.9}Ce_{0.1}Mn_{1-y}Cr_yO_3$ ($y = 0.00$, 0.05 and 0.10) compounds.

the basis of favoured growth of the FM phases at the expense of the AFM phases, when the compounds are cooled under magnetic field. These differences in the behaviours under FC and ZFC conditions have been compared with those exhibited by the 'diluted Ising antiferromagnets' with random impurities in their long range AFM structures [23]. It has been argued that during field cooling the long range AFM order breaks into domains with a favoured growth of the more conducting FM domains and leads to the observations of higher magnetization and conductivity than those observed under the zero-field-cooled (ZFC) condition. The observed

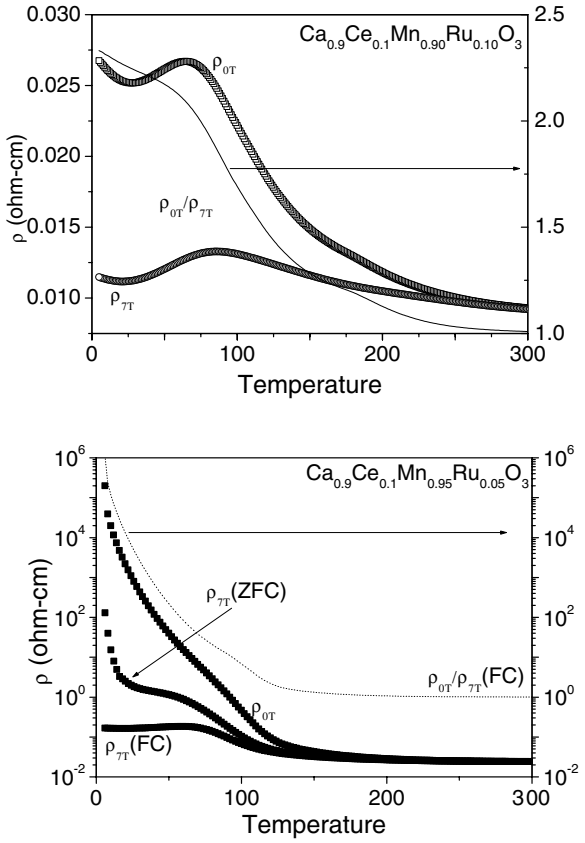

Figure 6. The DC electrical resistivity versus temperature plots of $Ca_{0.9}Ce_{0.1}Mn_{0.95}Ru_{0.05}O_3$ and $Ca_{0.9}Ce_{0.1}Mn_{0.90}Ru_{0.10}O_3$.

difference between the FC and ZFC plots decreases with increase in Cr and Ru concentration, and unlike what is observed from our DC magnetic studies, it is completely absent in the Ru-substituted $y = 0.10$ compound due to percolation of FM phases.

The ρ versus H plots of the Ru- and Cr-doped compounds, with CMR behaviours recorded at 15 K, under ZFC and FC conditions are shown in figure 7. The irreversible conversion of AFM phases to the FM phases, observed from the M–H behaviours of these compounds, is also reflected in their ρ–H plots (ZFC) as they exhibit large differences between their zero-field resistivities before and after field cycling in the path 0–7 T and then back to 0 T. Although the zero-field resistivities do not change upon further field cycling, a significant hysteresis is observed between the decreasing and the increasing paths of magnetic field. Since these compounds show very small remanent magnetizations, the observed remanence in their resistivities is clearly not related to the magnetic-field-induced alignment of the FM domains but only to the irreversible conversion of AFM to FM phases. Similar ρ–H behaviours have been reported in the literature for a number of manganites with co-existing FM and non-ferromagnetic phases [24–27, 36]. In the case of the FC plots, since the field-induced irreversible conversion of AFM to FM phases takes place while cooling under magnetic field, such remanence in resistivities is absent. Hysteresis between decreasing and increasing paths of magnetic field, however, does exist in these FC plots. As in the case of ρ–T plots, the FC

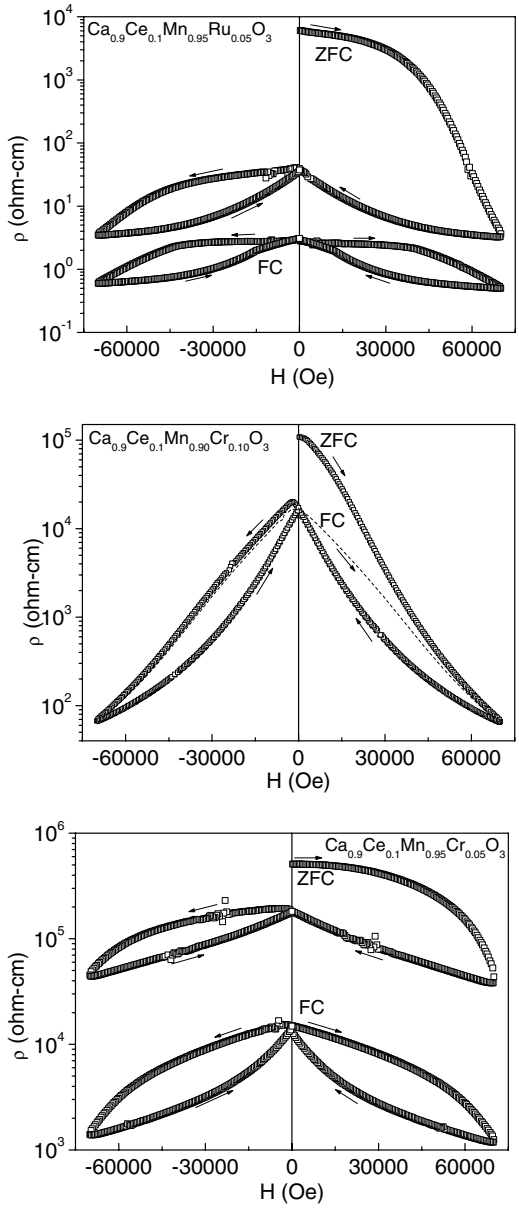

Figure 7. The DC electrical resistivity versus field plots of the $Ca_{0.9}Ce_{0.1}Mn_{1-y}Cr_yO_3$ ($y = 0.05$ and 0.10) and the $Ca_{0.9}Ce_{0.1}Mn_{0.95}Ru_{0.05}O_3$ compounds recorded at 15 K.

plots of $y = 0.05$ compounds show a much lower value of resistivities than the ZFC plots at all magnetic fields. The observed hysteresis in the ZFC and FC plots can be ascribed to the magnetic heterogeneity of these compounds, since similar hystereses have been observed in the ρ versus H plots of the compound $Pr_{0.7}Ca_{0.25}Sr_{0.05}MnO_3$ (at 88 K), with coexisting FM and AFM phases [36].

To understand the relaxation behaviours of resistivities of these compounds with respect to time and temperature, we recorded the remanent resistivity versus temperature and time plots

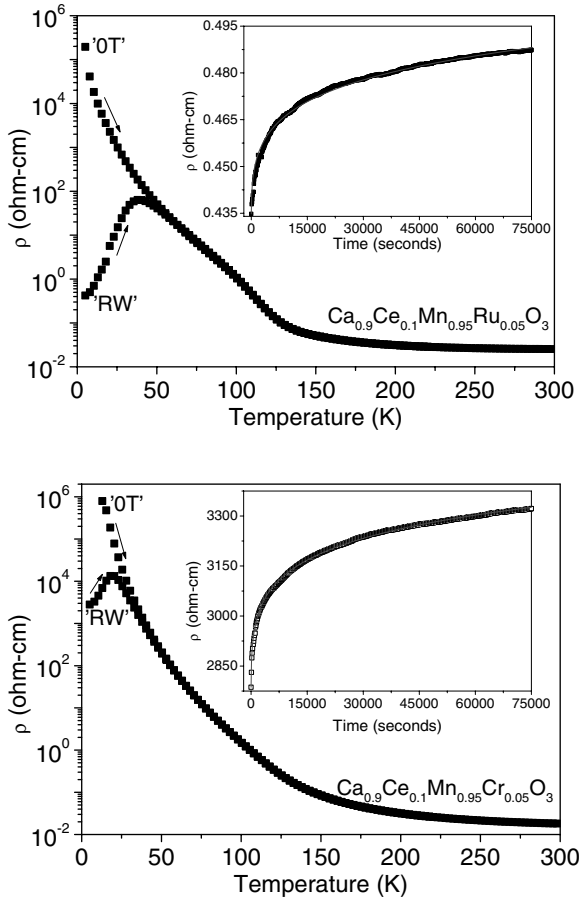

Figure 8. The DC electrical resistivity versus temperature plots of the $Ca_{0.9}Ce_{0.1}Mn_{0.95}Cr_{0.05}O_3$ and the $Ca_{0.9}Ce_{0.1}Mn_{0.95}Ru_{0.05}O_3$ compounds. '0 T' and 'RW' plots represent the 'zero-field' and 'remanent' resistivities, respectively, recorded during the warming cycle. The insets of the figures show the variation of the remanent resistivity with time at 5 K (the curve shows the fit to the data).

of $Ca_{0.9}Ce_{0.1}Mn_{0.95}Ru_{0.05}O_3$ and $Ca_{0.9}Ce_{0.1}Mn_{0.95}Cr_{0.05}O_3$ at 0 T magnetic field after field cooling them under 7 T magnetic field (figure 8). At the lowest temperature of measurement, the values of these remanent resistivities (termed as 'RW' in figure 8 and recorded while warming) are orders of magnitude lower than the values of the respective '0 T' resistivities (also recorded while warming). With an increase in temperature, they approach and become ultimately equal to the '0 T' resistivities at the point where the 'RW' and '0 T' plots merge with each other. The metal-like behaviours of these 'RW' plots are similar to that reported for the thin film form of the compound $Nd_{0.7}Sr_{0.3}MnO_3$ [26]. This magnetic-history-dependent effect, which has been termed the GMM effect [26], has been explained on the basis of the effect of magnetic field on the subtle balance between the FM metallic (FMM) phase and the paramagnetic insulating phase (PMI), with activated hopping behaviour. The reduced FM phase fractions in those FM $Nd_{0.7}Sr_{0.3}MnO_3$ films in which such 'GMM' effects were observed were evident from the much lower values of saturation magnetization they exhibited as compared to that observed in the bulk $Nd_{0.7}Sr_{0.3}MnO_3$ [41]. In the present case too, the magnetic-history-dependent balance between the FM and AFM phases is likely to give rise to

similar GMM effects. In the presence of the magnetic field during the field cooling process, the growth of the FM phases is favoured at the expense of the AFM phases. When the field is removed at low temperature, the FM phases, which are formed in the presence of the magnetic field, cannot lose their FM character immediately because of the high energy barrier they have to cross to go through that process. With increase in temperature, since crossing of the energy barrier becomes easier in the presence of an enhanced thermal energy, a decrease in the FM fraction leads to a decrease in the difference in the resistivity values between of the 'RW' and the '0 T' plots. The change in the remanent resistivity of these compounds at 5 K with increase in time is shown as the inset of the corresponding ρ–T plots in figure 8. In both the cases, the increase in resistivity is a very small fraction of the difference in the resistivity values between the 'RW' and '0 T' plots at 5 K. This shows that the time effect in the increase in resistivity with temperature for the 'RW' plot is insignificant. The exponential-like growth in resistivity observed for these compounds can be fitted quite well with the equation

$$\rho = \rho_0(1 + \exp(-(\tau/t)^{\beta})$$

(τ = characteristic relaxation time and β = dispersion parameter, the values of which are shown in table 1).

In the literature, a similar exponential function has been used to describe the decay of remanent magnetization with time for the layered manganite $(La_{0.4}Pr_{0.6})_{1.2}Sr_{1.8}Mn_2O_7$ [27]. From the measurements of the decay processes at different temperatures it has been shown that the characteristic decay time, τ, decreases exponentially and the dispersion parameter, β, increases linearly with an increase in the temperature of the measurements. In the present case, however, no such systematic variations of the values of τ and β are observed when the measurements are made at different temperatures. Since the relaxation of the remanent resistivity is likely to depend on factors of temperature as well as the difference between the resistivity values in the '0 T' and the 'RW' plots, this behaviour arises probably from two competing effects of increase in temperature, i.e. an increase in thermal energy and a decrease in the difference between the resistivity values in the '0 T' and the 'RW' plots.

In conclusion, a detailed study on the magnetic and transport properties of the $Ca_{0.9}Ce_{0.1}Mn_yM_yO_3$ (M = Cr, Ru) compounds has been carried out. As in the case of the $Ca_{0.8}Sm_{0.2}Mn_yM_yO_3$ (M = Cr, Ru) compounds, the present Cr- and Ru-doped compounds also show magnetic heterogeneity with co-existing FM and AFM phases. Such magnetic phase separation in them is reflected in the observations of cluster-glass-like behaviour, and a number of magnetic-history-dependent transport and magnetic properties, including the GMM effect. The observed GMM effect is the first of its kind in the magnetically phase-separated bulk polycrystalline compounds.

References

[1] Jin S, Tiefel T H, McCoack M, Fastnacht R A, Ramesh R and Chen L H 1994 *Science* **264** 413
[2] Von Helmolt R, Wecker J, Holzapfel B, Schultz L and Samwer K 1994 *Phys. Rev. Lett.* **7** 2331
[3] Martin C, Maignan A, Damay F, Hervieu M and Raveau B 1997 *J. Solid State Chem.* **134** 198
[4] Rao C N R, Cheetham A K and Mahesh R 1996 *Chem. Mater.* **8** 2421
[5] Coey J M D, Viret M and von Molnar S 1999 *Adv. Phys.* **48** 167
[6] Dagotto E, Hotta T and Moreo A 2001 *Phys. Rep.* **344** 1
[7] Koo T Y, Kiryukhin V, Sharma P A, Hill J P and Cheong S-W 2001 *Phys. Rev.* B **64** 220405
[8] Moreo A, Yunoki S and Dagotto E 1999 *Science* **283** 2034
[9] Kim K H, Uehara M, Hess C, Sharma P A and Cheong S-W 2000 *Phys. Rev. Lett.* **84** 2961
[10] Maignan A, Martin C, Damay F and Raveau B 1998 *Chem. Mater.* **10** 950
[11] Sunderasan A, Tholence J L, Maignan A, Martin C, Hervieu M, Raveau B and Suard E 2000 *Eur. Phys. J.* B **14** 431

[12] Martin C, Maignan A, Hervieu M, Raveau B, Jirak Z, Savosta M M, Kurbakov A, Trounov V, Andre G and Bouree F 2000 *Phys. Rev.* B **62** 6442
[13] Neumeier J J and Cohn J L 2000 *Phys. Rev.* B **61** 14 319
[14] Maignan A, Martin C, Damay F, Raveau B and Hejtmanek J 1998 *Phys. Rev.* B **58** 2758
[15] Hejtmánek J, Jirák Z, Maryško M, Martin C, Maignan A, Hervieu M and Raveau B 2000 *Phys. Rev.* B **60** 14 057
[16] Raveau B, Maignan A, Martin C and Hervieu M 1997 *J. Solid State Chem.* **130** 162
[17] Maignan A, Martin C and Raveau B 1999 *Mater. Res. Bull.* **34** 345
[18] Martin C, Maignan A, Hervieu M, Raveau B and Hejtmanek J 2000 *Eur. Phys. J.* B **16** 469
[19] Hervieu M, Martin C, Maignan A and Raveau B 2000 *J. Solid State Chem.* **155** 15
[20] Maignan A, Martin C, Hervieu M, Damay F and Raveau B 1998 *J. Magn. Magn. Mater.* **188** 185
Maignan A, Martin C, Hervieu M, Damay F and Raveau B 2000 *Solid State Commun.* **117** 377
[21] Kimura T, Tomioka Y, Kumai R, Okimoto Y and Tokura Y 1999 *Phys. Rev. Lett.* **83** 3940
[22] Mahendiran R, Hervieu M, Maignan A, Martin C and Raveau B 2000 *Solid State Commun.* **114** 429
[23] Mahendiran R, Maignan A, Martin C, Hervieu M and Raveau B 2000 *Phys. Rev.* B **62** 11 644
[24] Barratt J, Lees R, Balakrishnan G and McK Paul D 1996 *Appl. Phys. Lett.* **68** 424
[25] Anane A, Renard J-P, Reversat L, Dupas C, Veillet P, Viret M, Pinsard L and Revcolevschi A 1999 *Phys. Rev.* B **59** 77
[26] Xiong G C, Li Q, Ju H L, Bhagat S M, Loafland S E, Greene R L and Venkatesan T 1995 *Appl. Phys. Lett.* **67** 3031
[27] Gordon I, Wagner P, Moschalkov V V, Bruynseraede Y, Apostu M, Suryanarayanan R and Revcolevschi A 2001 *Phys. Rev.* B **64** 092408
[28] Levy P, Parisi F, Quintero M, Granja L, Curiale J, Sacanell J, Levya G, Polla G, Freitas R S and Ghivelder L 2002 *Phys. Rev.* B **65** 140401
[29] Algarabel P A, De Teresa J M, Garcia-Landa B, Morellon L, Ibarra M R, Ritter C, Mahendiran R, Maignan A, Hervieu M, Martin C and Raveau B 2002 *Phys. Rev.* B **65** 104437
[30] Zeng Z, Greenblatt M and Croft M 2001 *Phys. Rev.* B **63** 224410
[31] Martin C, Maignan A, Hervieu M, Autret C, Raveau B and Khomski D I 2001 *Phys. Rev.* B **63** 174402
[32] Shanon R D 1976 *Acta Crystallogr.* **32** 751
[33] Hervieu M, Barnabé A, Martin C, Maignan A, Damay F and Raveau B 1999 *Eur. Phys. J.* **8** 31
[34] Hervieu M, Martin C, Maignan A, Van Tendeloo G and Raveau B 1999 *Eur. Phys. J.* B **10** 397
[35] Martin C, Maignan A, Hervieu M, Raveau B, Jirak Z, Kurbakov A, Trounov V, Andre G and Bouree F 1999 *J. Magn. Magn. Mater.* **205** 184
[36] Maignan A, Simon C, Caignaert V and Raveau B 1996 *J. Magn. Magn. Mater.* **152** L5
[37] Nam D N H, Jonason K, Nordblad P, Khiem N V and Phuc N X 1999 *Phys. Rev.* B **59** 4809
[38] Mukherjee S, Ranganathan R, Anilkumar P S and Joy P A 1996 *Phys. Rev.* B **54** 9267
[39] De Teresa J M, Ibarra M R, Blasco J, Ritter C, Algarabel P A, Marquina C and Del Moral A 1996 *Phys. Rev. Lett.* **76** 3392
[40] Worledge D C, Mieville L and Geballe T H 1998 *Phys. Rev.* B **57** 15 267
[41] Nam D N H, Mathieu R, Nordblad P, Khiem N V and Phuc N X 2000 *Phys. Rev.* B **62** 1027